Available online at www.sciencedirect.com
ScienceDirect
Materials Chemistry and Physics 108 (2008) 160–164
MATERIALS CHEMISTRY AND PHYSICS
www.elsevier.com/locate/matchemphys

Growth and structural characterization of ZnO on Y_2O_3/YSZ by pulsed laser deposition

Chih-Wei Lin, Yen-Teng Ho, Li Chang *

Department of Materials Science and Engineering, National Chiao Tung University, Hsinchu 300, Taiwan

Received 12 January 2007; received in revised form 16 July 2007; accepted 19 September 2007

Abstract

Pulsed laser deposition was used to form epitaxial Y_2O_3 buffer layers on yttria-stabilized zirconia (YSZ) (1 1 1) substrates, followed by formation of epitaxial ZnO. Structural characterization by X-ray diffraction, atomic force microscopy, and transmission electron microscopy (TEM) shows that Y_2O_3 has high-quality crystalline characteristics with a smooth (1 1 1) surface, providing a good buffer for deposition of ZnO films on YSZ. For ZnO deposition, a two-step growth process had been adopted, which consisted of low-temperature nucleation and high-temperature growth. ZnO films on Y_2O_3/YSZ have good structural qualities in *c*-axis orientation with smooth surfaces. Electron diffraction patterns show an orientation relationship of $[2\,\bar{1}\,\bar{1}\,0]_{ZnO}//[0\,\bar{1}\,1]_{Y_2O_3}$ and $(0\,0\,0\,2)_{ZnO}//(2\,2\,2)_{Y_2O_3}$. High-resolution TEM clearly reveals that both the interfaces of ZnO/Y_2O_3 and Y_2O_3/YSZ are flat without the formation of any interlayers.

Keywords: Oxides; Epitaxial growth; Electron microscopy; Microstructure

1. Introduction

ZnO is an attractive oxide semiconductor material for optoelectronic applications such as short-wavelength light emitting diodes and laser diodes because of its superior properties of direct wide band gap (3.37 eV) and high exciton binding energy (60 meV). To fabricate high-quality ZnO thin films for devices, several growth techniques of ZnO have been used, including sputtering [1,2], molecular beam epitaxy (MBE) [3,4], pulsed laser deposition (PLD) [5,6] and chemical vapor deposition (CVD) [7,8]. PLD for deposition of metal oxide films has several advantages such as high-quality growth and accurate stoichiometry. It is of great interest to grow epitaxial ZnO on Si substrates as large wafers are commercially available at low costs. Epitaxial Y_2O_3 can be easily grown on Si (1 1 1) as Y_2O_3 ($a_0 = 1.0604$ nm, space group $Ia\bar{3}$) has a low lattice mismatch with Si ($a_0 = 0.543$ nm) [9,10]. Also, the mismatch of ZnO (wurtzite structure, $a_0 = 0.325$ nm, and $c_0 = 0.521$ nm) with Y_2O_3 is reasonable probably in the range of 7–14% along ZnO $[1\,1\,\bar{2}\,0]$ and Y_2O_3 [1 1 0] which depends on the surface structure. Therefore, it is possible to use Y_2O_3 as a buffer for deposition of epitaxial ZnO on Si. Nevertheless, there are some problems with the interlayer formation of silicon oxide between Y_2O_3 and Si for epitaxial growth of Y_2O_3 on Si substrate [11]. Our previous studies of ZnO films grown on Y_2O_3/Si substrate by MOCVD and PLD [12,13] showed that film growth was not optimal probably due to the formation of an interlayer of silicon oxide. To further evaluate the effect of Y_2O_3 on the structural qualities of deposited ZnO films, we have deposited Y_2O_3 on yttria-stabilized zirconia (YSZ) instead of Si. YSZ has the CaF_2-type cubic structure (space group $Fm\bar{3}m$) with lattice constant of 0.514 nm which gives a lattice mismatch of 3.15% with Y_2O_3. Other advantages for using YSZ substrates are that smooth single crystal substrates are available in high crystalline quality, and it is chemically compatible with Y_2O_3. Until now, the consequences of growth of Y_2O_3 films on YSZ(1 1 1) have been rarely reported. For the first time, we report the results of X-ray diffraction (XRD), atomic force microscopy (AFM), and cross-sectional transmission electron microscopy (TEM) which prove the growth of an epitaxial Y_2O_3 film on YSZ which can be used as a buffer layer for ZnO growth. We also present the results on ZnO films subsequently deposited on Y_2O_3.

2. Experimental procedures

Y_2O_3 films were deposited on YSZ(1 1 1) single crystal substrates by pulsed laser deposition. The base pressure of the growth chamber was below 1.33×10^{-6} Pa at room temperature. YSZ(1 1 1) substrates of 1 cm × 1 cm size

* Corresponding author. Tel.: +886 3 5731615; fax: +886 3 5724727.
E-mail address: lichang@cc.nctu.edu.tw (L. Chang).

0254-0584/$ – see front matter © 2007 Elsevier B.V. All rights reserved.
doi:10.1016/j.matchemphys.2007.09.033

were cleaned with acetone before loading into the growth chamber. Further surface cleaning of YSZ substrates was done by annealing at 900 °C for 30 min in vacuum. A KrF excimer laser with wavelength of 248 nm was used with a pulse rate of 3 Hz for ablation of a Y_2O_3 ceramic target (99.99% purity). The substrate temperature was 850 °C, and the oxygen pressure was maintained at 4 Pa during deposition of Y_2O_3. O_2 gas (99.999% purity) was used as oxygen source for deposition of Y_2O_3 and ZnO. After deposition of Y_2O_3 buffer layer, a ZnO film was immediately deposited by PLD in the same growth chamber. ZnO deposition was performed in a two-step process. First, a low-temperature (LT) ZnO nucleation layer was deposited at 450 °C for 10 min. Then, ZnO growth was performed at high temperature (HT) of 750 °C for 120 min. During ZnO deposition, the oxygen pressure was kept at 1.33 Pa and the laser pulse rate was 5 Hz for ablation of a ZnO ceramic target (99.99% purity). Crystalline qualities and orientations of films were evaluated by XRD, and surface morphologies were examined by AFM. The thickness and microstructure of films were characterized using cross-sectional TEM.

3. Results and discussions

3.1. Y_2O_3 films grown on YSZ(1 1 1) substrates

Fig. 1(a) is a typical XRD pattern in θ–2θ scan from a Y_2O_3 film on YSZ which shows only the (2 2 2) reflection of Y_2O_3 in addition to the reflections of YSZ. It suggests that Y_2O_3 films have a (1 1 1) oriented surface parallel to (1 1 1) planes of YSZ substrate. The Y_2O_3 (2 2 2) X-ray rocking curve in Fig. 1(b) shows the full-width half maximum (FWHM) of 190 arcs, implying that the Y_2O_3 film is of good crystalline quality. AFM shows that the surface roughness (rms) is about 0.3 nm for the

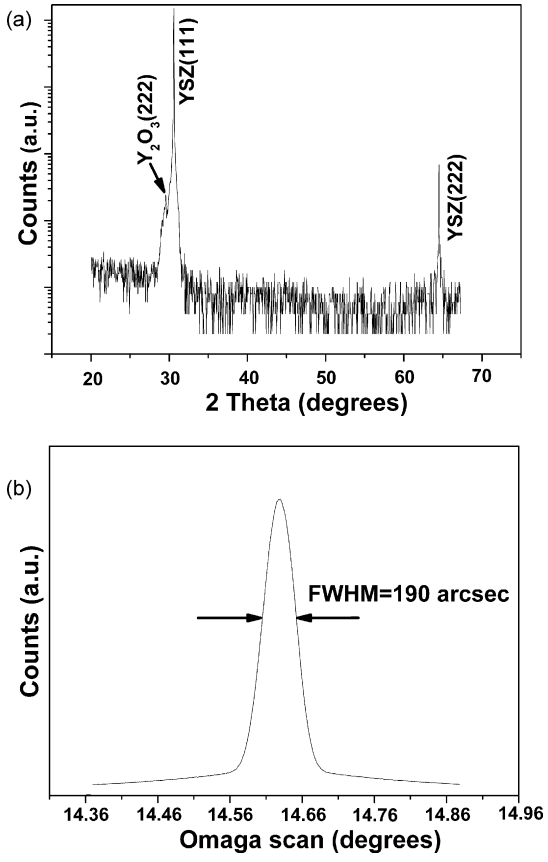

Fig. 1. (a) θ–2θ scan XRD diagram of Y_2O_3 on YSZ(1 1 1) substrate. (b) Rocking curve of the (2 2 2) reflection of Y_2O_3 on YSZ(1 1 1) substrate.

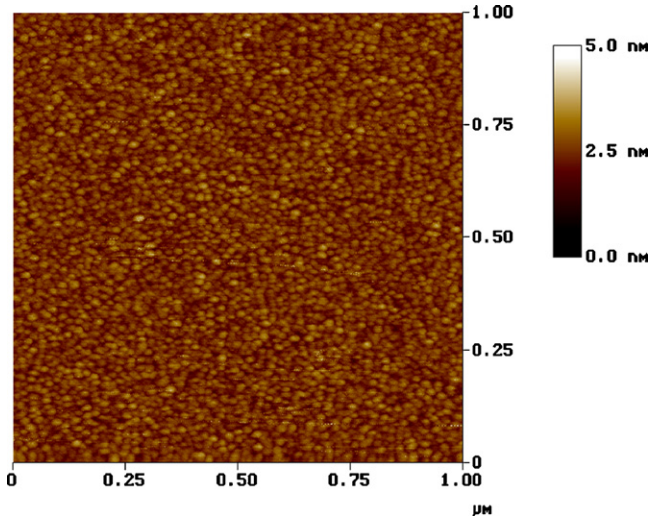

Fig. 2. Typical AFM image of Y_2O_3 grown on YSZ(1 1 1) substrate.

Y_2O_3 films as seen in Fig. 2 for a typical case, indicating smooth and flat surfaces. The surface roughness value is close to that of as-received YSZ substrates. Fig. 3(a) shows a bright-field TEM image of Y_2O_3 on YSZ substrate. The uniform image contrast of the Y_2O_3 film suggests that a large number of grains are well

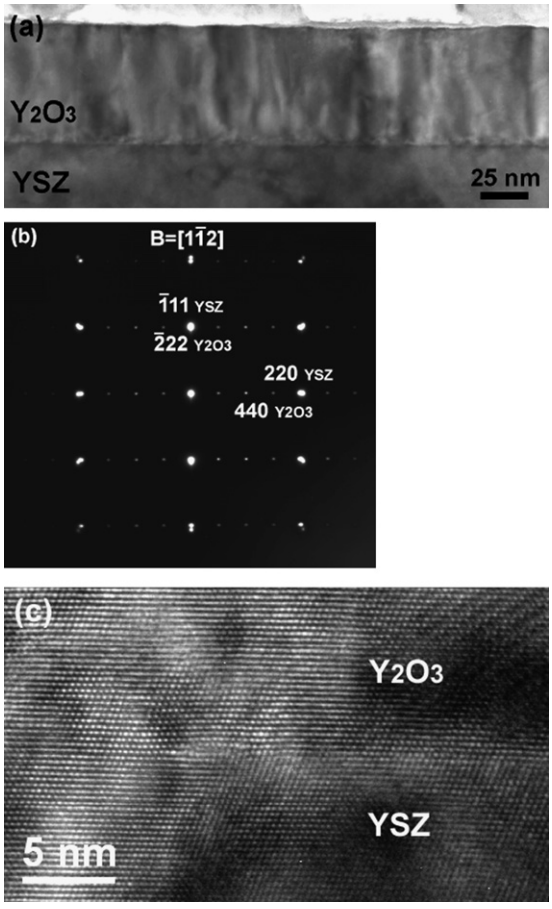

Fig. 3. (a) Cross-sectional bright-field TEM image of Y_2O_3 on YSZ, and (b) the corresponding electron diffraction pattern in [1 $\bar{1}$ 2] zone axis. (c) HRTEM image of the interface between Y_2O_3 and YSZ along the [1 $\bar{1}$ 0] zone axis.

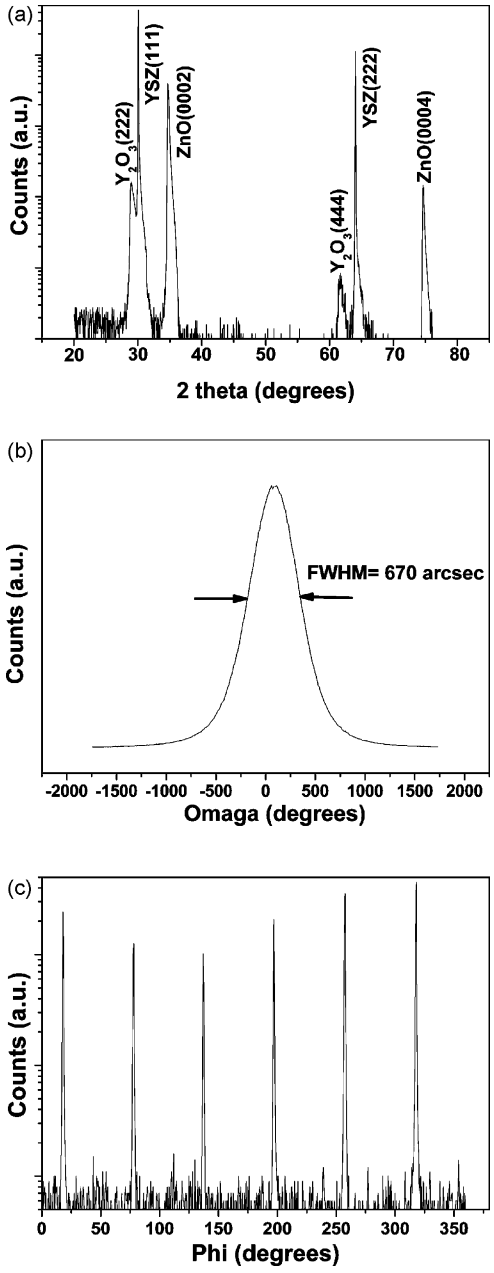

Fig. 4. (a) θ–2θ scan XRD diagram of ZnO on Y_2O_3/YSZ substrate. (b) (0 0 0 2) Rocking curve of ZnO on Y_2O_3/YSZ substrate. (c) (1 0 $\bar{1}$ 3) Phi-scan of ZnO on Y_2O_3/YSZ substrate.

aligned in the in-plane direction. The selected area diffraction (SAD) pattern in Fig. 3(b) acquired at the interface region containing Y_2O_3 and YSZ reveals the good epitaxy between them. The orientation relationship of Y_2O_3 and YSZ is determined as $[1\,\bar{1}\,2]_{Y_2O_3}//[1\,\bar{1}\,2]_{YSZ}$ and $[\bar{2}\,2\,2]_{Y_2O_3}//[\bar{1}\,1\,1]_{YSZ}$ The thickness of the Y_2O_3 film as measured by TEM is about 67 nm, yielding a growth rate of 0.037 nm/s. Fig. 3(c) is a cross-sectional high-resolution TEM image of the interface between Y_2O_3 and YSZ along the $[1\,\bar{1}\,0]$ direction. It is clearly observed that the interface is atomically flat and smooth with good coherency between Y_2O_3 and YSZ as evident from (2 2 2) lattice fringes of Y_2O_3 parallel to (1 1 1) ones of YSZ in the image. From the

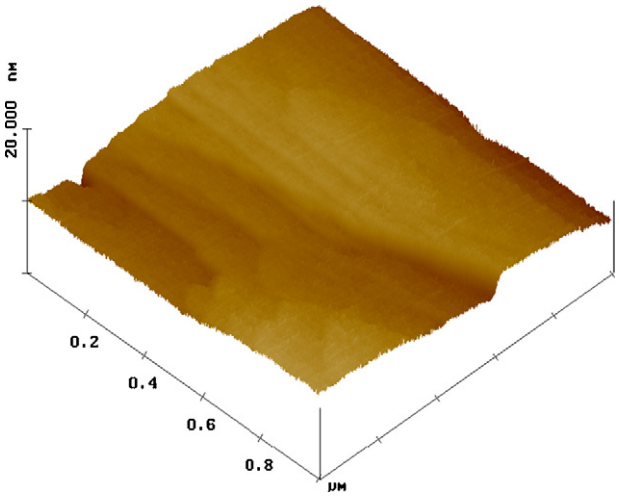

Fig. 5. Typical AFM image of ZnO grown on Y_2O_3/YSZ substrate.

above results of structural characterization, the deposited Y_2O_3 films can serve as a buffer layer for ZnO deposition.

3.2. ZnO films grown on Y_2O_3/YSZ(1 1 1) substrates

Subsequently, ZnO films were deposited on Y_2O_3/YSZ substrates in a two-step growth process, consisting of a LT-ZnO nucleation layer and a HT-ZnO layer. Fig. 4 shows the XRD results of the ZnO layers in θ–2θ, (0 0 0 2) rocking curve, and (1 0 $\bar{1}$ 3) phi-scan patterns. On the θ–2θ scan shown in Fig. 4(a), only (0 0 0 2) and (0 0 0 4) peaks of ZnO are observed, implying c-axis growth of ZnO on Y_2O_3/YSZ substrate. The FWHM of the ZnO (0 0 0 2) peak is 670 arcs from the rocking curve pattern shown in Fig. 4(b), suggesting that ZnO films of good crystallinity are obtained. In comparison with our previous results of ZnO on Y_2O_3/Si which showed the FWHM value larger than 0.5°, the crystallinity of the ZnO films on YSZ is much improved. To investigate the in-plane symmetry of the ZnO layers, we used ZnO (1 0 $\bar{1}$ 3) plane for phi-scan characterization. In the phi-scan range of 0–360 degrees [shown in Fig. 4(c)], we can see six peaks which are mutually separated by 60° with the FWHM of each peak in the range of 0.6–0.9°, suggesting that ZnO grains are well aligned with each other. Fig. 5 shows the AFM surface morphology of a ZnO film which may result from 3D island growth. However, atomically flat terraces are clearly seen with steps which have a height of about 0.5 nm corresponding to the length of the c-axis of ZnO. The averaged surface roughness (rms) of ZnO is 0.92 nm, implying that the surface of the ZnO film grown on Y_2O_3 by PLD is quite flat. Fig. 6(a) shows a bright-field TEM image of the ZnO and Y_2O_3 layers on YSZ, and Fig. 6 (b) shows the corresponding SAD pattern of the ZnO and Y_2O_3 layers along the $[0\,\bar{1}\,1]$ zone axis of Y_2O_3. The measured thickness of the ZnO film from the TEM image is about 595 nm from which an averaged growth rate of 0.076 nm/s for ZnO deposition is determined. It is of interest to notice that there is a relatively low density of dislocations in the top half part of the ZnO film. The roughly estimated dislocation density is about 2×10^9 cm^{-2}. From the SAD pat-

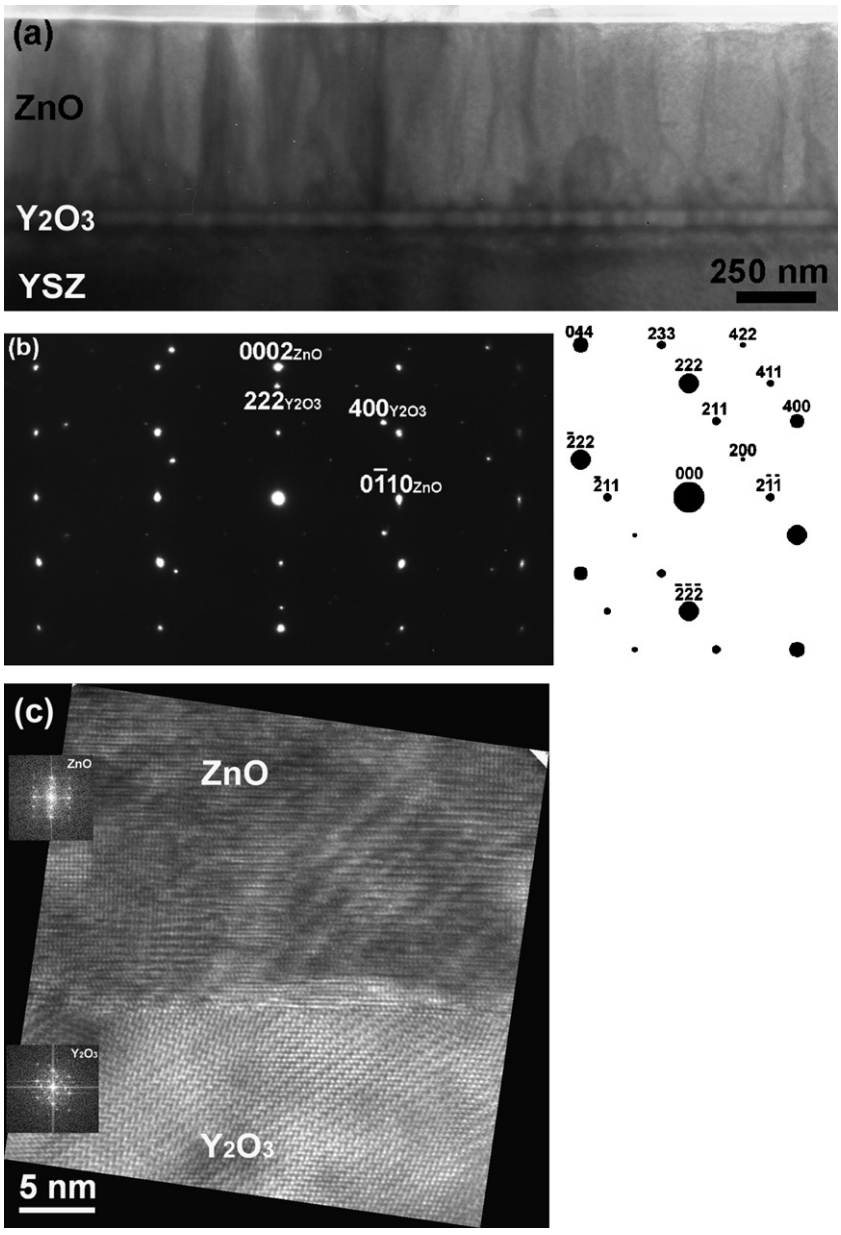

Fig. 6. (a) Cross-sectional bright-field TEM image of ZnO on Y_2O_3/YSZ, and (b) the corresponding electron diffraction pattern of the ZnO and Y_2O_3 layers in [0 $\bar{1}$ 1] zone axis with indexed Y_2O_3 reflections. (c) HRTEM image of the interfacial region between ZnO and Y_2O_3 along the [0 1 $\bar{1}$] zone axis with FFT patterns of ZnO and Y_2O_3.

tern in Fig. 6(b), the [0 $\bar{1}$ 1] zone axis of Y_2O_3 is parallel to the [2 $\bar{1}$ $\bar{1}$ 0] zone of ZnO, and the (2 2 2) plane of Y_2O_3 is parallel to (0 0 0 2) of ZnO. Therefore, the orientation relationship between ZnO and Y_2O_3 can be deduced as $[2\,\bar{1}\,\bar{1}\,0]_{ZnO}//[0\,\bar{1}\,1]_{Y_2O_3}$ and $(0\,0\,0\,2)_{ZnO}//(2\,2\,2)_{Y_2O_3}$. Fig. 6(c) is a high-resolution TEM image of the interface between ZnO and Y_2O_3 with fast-Fourier-Transform (FFT) patterns from ZnO and Y_2O_3. In addition, from the FFT and SAD patterns, the Y_2O_3 (4 $\bar{2}$ $\bar{2}$) and ZnO (0 $\bar{1}$ 1 0) planes are parallel in in-plane orientation with *d*-spacings of 0.216 and 0.284 nm, respectively, which gives a ratio close to 3:4. Therefore, it is likely to obtain in-plane epitaxial relationship for ZnO on Y_2O_3 along the [2$\bar{1}\bar{1}$] direction. The interface between ZnO and Y_2O_3 is sharp, and no reaction interlayers can be detected, which is similar to our previous report of the ZnO/Y_2O_3 films on Si [12,13]. The above results confirm that ZnO can be epitaxially grown on Y_2O_3 with good structural qualities. For epitaxial growth of ZnO on Si (1 1 1) using Y_2O_3 buffer layer, it is expected that high-quality ZnO films can be obtained if the formation of the interlayer between Y_2O_3 and Si is inhibited.

4. Conclusions

Deposition of epitaxial Y_2O_3 films on YSZ (1 1 1) substrates by PLD has been demonstrated. High-quality (2 2 2) Y_2O_3 films on YSZ can be achieved with smooth surfaces, which provide good buffer layer for subsequent deposition of ZnO. On the Y_2O_3 films, high-quality epitaxial ZnO films can be success-

fully deposited. The ZnO films are shown to be strongly *c*-axis oriented with good in-plane alignment, and they exhibit a 3D island surface morphology with flat terraces. Furthermore, the deposited ZnO films have a relatively low density of dislocations, and the interface with Y_2O_3 is smooth without the formation of any interlayers as well. The orientation relationship between ZnO and Y_2O_3 can be characterized as $[2\,\bar{1}\,\bar{1}\,0]_{ZnO}//[0\,\bar{1}\,1]_{Y_2O_3}$ and $(0\,0\,0\,2)_{ZnO}//(2\,2\,2)_{Y_2O_3}$.

Acknowledgements

This work was supported in part by National Science Council, Taiwan, ROC, under Contract NSC 95-2221-E-009-128.

References

[1] C.H. Choi, S.H. Kim, J. Crystal Growth 283 (2005) 170.
[2] I.S. Kim, S.H. Jeong, S.S. Kim, B.T. Lee, Semicond. Sci. Technol. 19 (2004) L29.
[3] T. Onuma, S.F. Chichibu, A. Uedono, Y.-Z. Yoo, T. Chikyow, T. Sota, M. Kawasaki, H. Koinuma, Appl. Phys. Lett. 85 (2004) 5586.
[4] X.Q. Wang, Y. Tomita, O.H. Roh, M. Ohsugi, S.B. Che, Y. Ishitani, A. Yoshikawa, Appl. Phys. Lett. 86 (2005) 011921.
[5] H. Zhao, L.Z. Hu, Z.Y. Wang, Z.J. Wang, H.Q. Zhang, Y. Zhao, X.P. Liang, J. Crystal Growth 280 (2005) 455.
[6] X.M. Fan, J.S. Lian, Z.X. Guo, H.J. Lu, Appl. Surf. Sci. 239 (2005) 176.
[7] Y.F. Chen, F.Y. Jiang, L. Wang, C.D. Zheng, J.N. Dai, Y. Pu, W.Q. Fang, J. Crystal Growth 275 (2005) 486.
[8] Y. Kashiwaba, H. Kato, T. Kikuchi, I. Niikura, K. Matsushita, Y. Kashiwaba, Appl. Surf. Sci. 244 (2005) 373.
[9] M.E. Hunter, M.J. Read, N.A. El-Marsy, J.C. Roberts, S.M. Bedair, Appl. Phys. Lett. 76 (2000) 1935.
[10] M.-H. Cho, D.-H. Ko, Y.K. Choi, I.W. Lyo, K. Jeong, T.G. Kim, J.H. Song, C.N. Whang, J. Appl. Phys. 89 (2001) 1647.
[11] S. Stemmer, D.O. Klenov, Z. Chen, D. Niu, R.W. Ashcraft, G.N. Parsons, Appl. Phys. Lett. 81 (2002) 712.
[12] C.W. Lin, T.Y. Cheng, L. Chang, J.Y. Juang, Phys. Stat. Sol. (c) 1 (2004) 851.
[13] C.W. Lin, T.Y. Cheng, L. Chang, J.Y. Juang, J. Crystal Growth 275 (2005) e2481.